Kragujevac J. Sci. 44 (2022) 25–36. UDC 537.311.3:773.2:591.471.24
doi: 10.5937/KgJSci2244025A *Original scientific paper*

COMPARATIVE STUDY OF ELECTRICAL RESISTANCE OF DISC-SHAPED COMPACTS FABRICATED USING CALCINED CLAMS SHELL, PERIWINKLE SHELL AND OYSTER SHELL NANOPOWDER

Adebayo Olusakin Adeniran[1], Akaninyene Okon Akankpo[1], Sunday Edet Etuk[1], Ubong Williams Robert[2], Okechukwu Ebuka Agbasi[3]*

[1]*University of Uyo, Department of Physics, Uyo, Nigeria*
[2]*Akwa Ibom State University, Department of Physics, Ikot Akpaden, Mkpat Enin, Nigeria*
[3]*Michael Okpara University of Agriculture, Department of Physics, Umudike, Nigeria*
*****Corresponding author; E-mail: agbasi.okechukwu@gmail.com

(Received December 04, 2021; Accepted February 2, 2022)

ABSTRACT. In this investigation, Clam, Periwinkle and Oyster shells were separately treated, calcined and ball-milled into nano powder. Each nano powder material was fabricated into disc of various lengths in three replicates. In each case, the electrical characteristics of the discs were determined. Electrical resistivity values obtained for test samples developed from Clam, Periwinkle and Oyster shells were found to be $(6.024 \pm 0.009) \times 10^5$ Ωm, $(6.823 \pm 0.030) \times 10^5$ Ωm, and $(4.916 \pm 0.007) \times 10^5$ Ωm respectively at a temperature of (25.0 ± 1.0^oC). Also, electronic activation energy values were found to be 0.68eV, 0.61eV, and 0.76eV, while thermal sensitivity index values were obtained as 7850K, 7058K, and 8814K respectively for the samples fabricated from the shells of Clam, Periwinkle, and Oyster. The shell samples exhibit a negative temperature coefficient of resistance with values of -8.83%/K, -7.94%/K and -9.92%/K for Clam, Periwinkle and Oyster shells respectively. These results provide data base on the electrical characteristics for the shells. It can be adjudged from the results that the shells are potential raw materials for NTC thermistor production. They have high sustainability and can be considered to be economically cheap since they are discarded as waste.

Keywords: Carr's compressibility index, electrical resistivity, electronic activation energy, thermal sensitivity, temperature coefficient.

INTRODUCTION

Ocean, sea, river and lake are our divine treasures. They are the sources of raw material, minerals, food, water, income and wealth in addition to the provision of the route for transportation. Calm, Periwinkle, and Oyster are some of the shellfish found in our estuary and lake. Their bodies are edible and they are sources of protein and iron whereas the shells are left mostly unused to pollute the environment due to the fact that they are not easily degradable.

These organisms are also regarded as marine snails, edible sea animals and marine gastropods (ADEWUYI and ADEGOKE, 2008).

Oyster shell dust, according to BUNJAMIN and MUKKLIS (2020), contains CaO which gives its grain higher compressive strength. Oyster shell is characterized by a high percentage (98.2%) of Calcium Carbonate content (HAMESTER *et al.*, 2012). COLOMA *et al.* (2006) reported on the use of Calcium Fluoride (CaF_2) from Oyster shells as a raw material for thermoluminescence dosimeter. KIM *et al.* (2020) indicated that Oyster shells can be used as an efficient sorbent for fluoride removal for the purpose of re-use of waste products.

In the case of Clam, TUROLLA *et al.* (2020) reported that marine aquaculture has tremendous potential to assist feed the teeming human population sustainability. Clams, and others in this case including Periwinkle are marine aquaculture of bivalve shellfish. The report of LIANG *et al.* (2016) confirmed $CaCO_3$ as the component of layers of Clamshell. This is collaborated by the report of MA *et al*. (2012). Clam, a bivalve mollusk, is found in abundance in seas in countries of West Africa (AJEI-BOATENG *et al*., 2009; ADEYEMO *et al*., 2013; AKINJOGUNLA and MORUF, 2018). KINGDOM *et al.*, (2012), EHIGIATOR and OSAWARU (2016) gave the length of Clamshell as 70.1 ± 3.4 mm and 63.26 ± 0.50 mm.

ADEWUYI and ADEGOKE (2008) reported on Periwinkle as a shellfish, describing it as a marine snail, having a spiral shell conical in nature with a round aperture which can grow to have a shell of 52 mm. Their report has shown that Periwinkle is used for food whereas the hard shell is seldom utilized but mostly left as waste. MA *et al.* (2012) equated $CaCO_3$ composition in Periwinkle shell to that of limestone. Their report has seen shell from shellfish as a natural layered composite material, having excellent performance determined by the ranking structure and organic matter that make up the shell. The percentage of $CaCO_3$ in the Periwinkle shell is reported to be above 70% (ONUOHA *et al.* 2017) up to 93.9% (OBOT *et al.*, 2017).

Even with this, the shells have no main use but are found littered around homes and markets. Efforts are made towards plausible ways waste recycling for beneficial use and re-use could be put to, in order to keep the environment tidy (ATUANYA *et al.*, 2014). Our research is predicated based on the above, with the aim of investigating the electrical characteristics of samples fabricated using nanopowder of Clam, Periwinkle, and Oyster shells for the purpose of establishing their potential as raw materials and necessary data base for industrial utilization.

THEORY

The electric field E as well as the property of a conducting material determines the current density J in the material. However, the dependency can appear to be very complex. In metals and some other materials, the current density at a given temperature is directly proportional to the electric field, leaving the ratio of electric field to current density a constant. This can be mathematically defined (YOUNG and FREEDMAN, 2008; ETUK *et al.*, 2021) thus

$$\rho = \frac{E}{J} \tag{1}$$

Hence, with a conductor having ρ as its resistivity, we have

$$E = \rho J \tag{2}$$

The above defines the resistivity, ρ of a material and is equally expressed as (SEDHA, 2008)

$$\rho = \frac{RA}{L} \tag{3}$$

where R = electrical resistance of the material, A = cross-sectional area of the material and L = length/thickness of the material.

Resistivity is also defined mathematically (THERAJA and THERAJA, 2005; THERAJA, 2012) as

$$\rho = \frac{1}{\cap e \mu_c} \tag{4}$$

where $\cap$ = number of free electrons per unit volume of the conductor/electron density, e = electron charge and μ_c = electron mobility.

A material that exhibits a linear relationship between an applied voltage and the corresponding current produced is regarded as a linear or an ohmic conductor and such is said to obey Ohm's law. Ohmic materials have constant resistivity at a given temperature and their mathematical relationship suffices thus

$$R = \frac{V}{I} \tag{5}$$

where V = applied voltage and I = the corresponding current produced.

It is obvious that the resistivity of a metallic material varies with temperature T since the resistance of a definite conductor equally varies especially at low temperatures. Ions of a conductor vibrate with greater amplitude as temperature increases, causing a moving electron and an ion to collide with each other and consequently impeding the drift of electrons passing through the conductor. In effect, this causes a reduction in current. The dependency of resistivity on temperature below 100°C can be expressed mathematically (SCHERZ and MONK, 2016) thus

$$\rho(T) = \rho_o[1 + \alpha(T - T_o)] \tag{6}$$

Resistance is equally known to vary with temperature. The variation is to be linear within certain ranges of temperature, a situation that gives rise to a relationship such as given by several authors including EKPE (2005), YOUNG and FREEDMAN (2008) thus

$$R(T) = R_o[1 + \alpha(T - T_o)] \tag{7}$$

where $R(T)$ = electrical resistance at temperature T, R_o = resistance at temperature T_o (where T_o is the temperature within 0 – 20°C), and α = temperature coefficient of resistance.

Whereas MORRIS (1996) expressed the temperature coefficient of resistance of a conductor at temperature θ_1 as

$$R_1 = R_o(1 + \alpha_o\theta_1) \tag{8}$$

R_o being the resistance of the conductor at 0°C; α_o is the temperature coefficient of resistance of the material referred to at θ°C.

EKPE and DEW (2002, 2004), and EKPE (2005) however expressed the temperature – resistance of a material as a power series thus

$$R(T) = R_o\big(1 + \alpha(T - T_o)\big) + \beta(T - T_o)^2 + \gamma(T - T_o)^3 + \cdots \tag{9}$$

defining R_o as the resistance of the material at a reference temperature, $T - T_o$; α, β and γ as material-related constants.

Considering the effect, the variation it causes on electrical quantities differs from one class of material to another. In some materials, a decrease in the levels of temperature results to increase in the value of electrical quantity whereas in some other classes of materials the situation is the reverse. It is based on this that the effect of temperature on electrical resistivity as well as thermal sensitivity index for a device made using such material can be expressed by an equation given by LUO *et al.* (2009)

$$\rho = \rho_o exp\left[\frac{E_a}{kT}\right] \tag{10}$$

where ρ_o = electrical resistivity at infinite temperature, T = absolute value of the select temperature, E_a = electronic activation energy, k = Boltzmann's constant, and β = thermal sensitivity index ($\beta = \frac{E_a}{k}$).

Considering eqs. 3 and 10 we arrive at an exponential approximation showing how electrical resistance relates to temperature T as given by MUNIFAH *et al.* (2018) and ROBERT *et al.* (2020), thus

$$\mathrm{R} = R_o exp\left[\frac{\beta}{T}\right] \tag{11}$$

and

$$\beta = \frac{E_a}{k} \tag{12}$$

For a small range of temperature, the thermal sensitivity (β-value) can be obtained for the device using the equation

$$\beta = T_2\left(\frac{T_1}{T_2 - T_1}\right) ln\left(\frac{R_1}{R_2}\right) \tag{13}$$

where R_1 and R_2 represent the values of electrical resistance recorded at temperatures T_1 and T_2 respectively.

Considering the above, the change in the device's resistance for a unit change in temperature, technically termed *the temperature coefficient of resistance* for the device can be estimated by employing the equation

$$\alpha = \pm\left[\frac{1}{R_1}\left(\frac{R_2 - R_1}{T_2 - T_1}\right)\right] 100\% \tag{14}$$

yielding (Robert et al., 2020)

$$\alpha = \pm\left(\frac{\beta}{T^2}\right) 100\% \tag{15}$$

(in which case the negative sign is used only if R varies inversely with T).

EXPERIMENTAL PROCEDURE

Materials collection and description

Shells of Clams, Periwinkle, and Oyster (Figure 1) discarded as waste materials were utilized in this work. They were gathered in large quantities from market dumpsites. The materials were sourced within the Uyo metropolis in Akwa Ibom State, Nigeria. Clean water from the water tap and distilled water were also used.

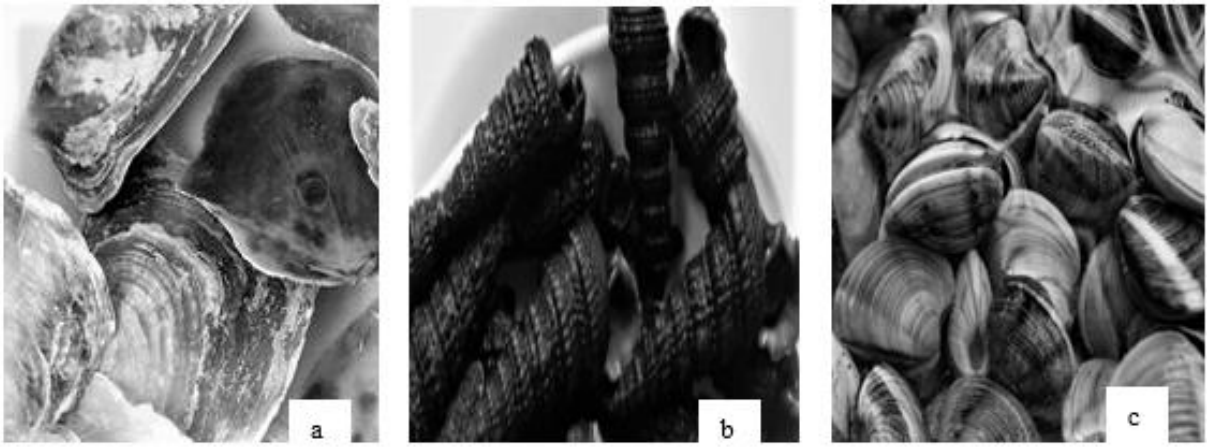

Figure 1. As-collected shells of Clam (a), Periwinkle (b) and Oyster (c).

Treatment and Processing of the waste materials (shells)

The shells were sorted, firstly washed with clean tap water to remove any dirt/impurities from them, and then immersed in Sodium hydroxide solution to be decolorized. They were then washed again using distilled water. After that, they were allowed to dry under ambient conditions before they were ground separately based on their type. Each category of the crushed materials was screened and the quantity that passed through 300 μm mesh openings was calcined in a Muffle ASCO furnace at 1000^{o}C for four hours. By means of a high-energy ball miller (E_{max} manufactured by RETSCH, GmbH), the calcined materials were further pulverized into nano powder at 500 rpm for six hours. This machine can ensure that the reduction in particle sizes of material feed is as fine as less than 80 nm from about 5 mm. By employing the standard procedure outlined in ASTM D6393 (2021), five determinations of Carr's Compressibility Index were made for each calcined nanomaterial. In each case, the mean and standard error values were calculated. For ease of identification, the nanopowders prepared from Clam shells, Periwinkle shells, and Oyster shells were coded as CSN, PSN, and OSN respectively.

Fabrication of test samples

The CSN was blended into a wetting liquid (Viscosity = 9.5 x 10^{-4} Pas) in a 6:1 weight ratio of the powder to the solution. The resulting homogeneous mixture was compacted to a diameter of (15.0 ± 0.1) mm by uniaxial pressing at 7.0 x 10^{2} N/m^{2} for 30 minutes. Then after, the pressed material was removed and sintered in air at 950^{o}C for two hours before it was diced into disc-shaped chips of various thicknesses. Three replicate discs were prepared per thickness. Other discs were similarly and separately fabricated from the PSN and OSN.

Testing of the prepared samples (Disc-shaped compacts)

At a time, one disc was engaged in a holder consisting of two lead terminals and a unit for the assemblage of a disc-shaped component. The terminals of the assembly were then connected to an LCR meter (Model 9183, Lutron) for electrical resistance measurements. All the developed samples, in each case, were tested and the mean resistance value was computed with the corresponding standard error per thickness (length) of the discs.

For investigation of the variation of electrical resistance with temperature, discs of thickness 4.0 mm were used. The temperature was monitored and measured over a range of 20°C to 50°C by means of a digital thermometer (calibrated and equipped with a type-K probe/sensor). Figure 2 shows the set-up diagrams for the measurements. In this work, nine

identical cylindrical copper cans (one for each trial, totaling three for the replicate samples of a particular nanopowder) were used.

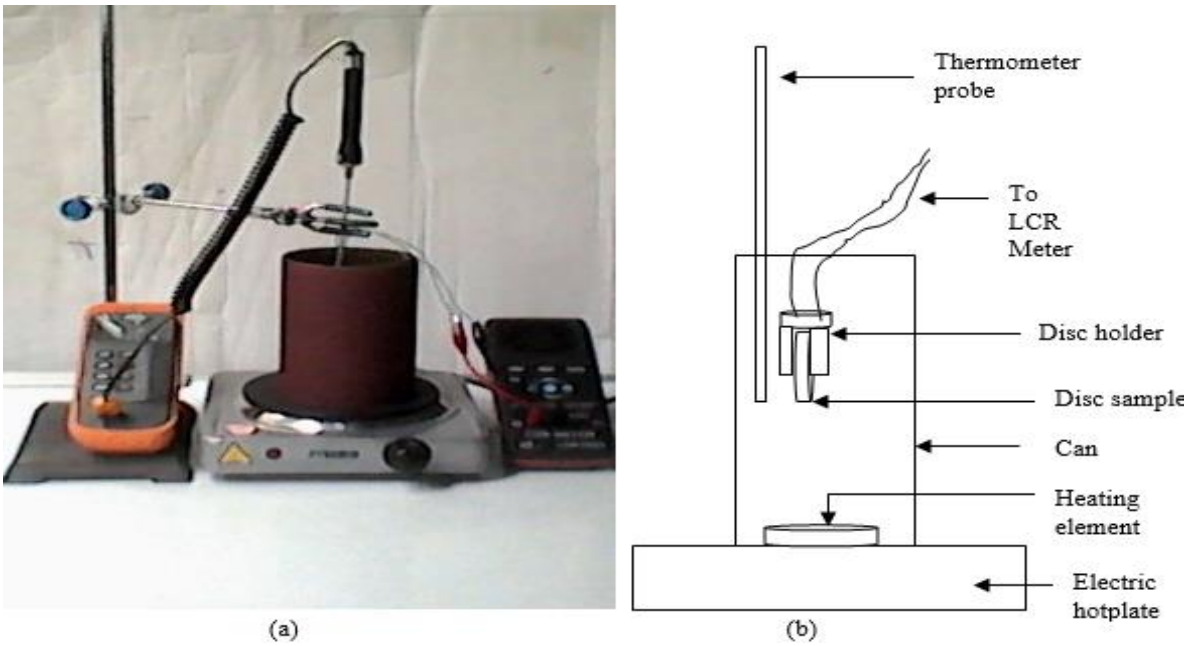

Figure 2. Set-up diagrams: Experimental (a) and Schematic (b).

The cans were carefully selected, ensuring that their open end fitted properly with the heating element of the electric hotplate. Pilot holes were provided at the closed (upper) end of each can for the accommodation of the assembly's lead wires and thermometer probe. The disc holder was thickly lagged with cotton wool to ensure that only the exposed portion of the disc was influenced by heat generated inside the can. Also, it was ensured that the exposed edge of the disc and tip of the probe was at the same level of suspension, which was maintained throughout the measurement process. By means of the control dial, the hotplate was regulated to a reasonable level which enabled its heating element to supply heat at a gradually increasing rate, causing a corresponding rise in the temperature of the disc. For each disc material, the mean values of electrical resistance were determined per temperature.

From the plot of electrical resistance against the thickness (length) of the disc in each case, the electrical resistivity was deduced based on the relation expressed as eq. 3. Also, from the plot of $ln\,R$ against the inverse of absolute temperature values, the thermal constant and then electronic activation energy and temperature coefficient of resistance were deduced in line with eqs. 11, 12, and 15 respectively.

RESULTS AND DISCUSSION

The characteristic forms of the ball-milled materials used in this study are shown in Table 1. It is obvious from the results that the powdery samples in all the cases have Carr's index value below 11%, hence, exhibit good flowability. This is an indication of good compressibility and the effect displays a good demonstration of bulk powder flow properties.

Carr's index, form and particle size are among the parameters considered to be very important in the fabrication or formulation of compressible pellets, tablets, or cubes as well as electronic components. The values of Carr's index and particle size obtained for the nanomaterials used in this study suggest that the materials are adequate for good fabrication. This is so adjudged because of the inverse relationship of flowability with compressibility.

Table 2 outlines the experimental results for resistance values per length of the disc samples. It can be observed from the values that samples fabricated using PSN exhibit the highest resistance values, followed by samples made from the CSN while those developed using the OSN have the lowest electrical resistance values. However, one-way analysis of the variance test between the various pairs yields F – values that show insignificant differences at $p < 0.05$. Figure 3 illustrates the variation of *R* with *L*, showing that the trend is linear in all the cases.

Table 1. Characteristic parameters of the ball-milled materials.

	Observation per material type		
Parameters	**CSN**	**PSN**	**OSN**
Carr's index (%)	10.63 ± 0.06	10.81 ± 0.04	1.78 ± 0.02
Form	Powdery	Powdery	Powdery
Particle size (nm)	≤ 80	≤ 80	≤ 80

Table 2. Outline of the determined experimental results for the material samples.

Material type	**Sample length, L (mm)**	**R values ($10^6\Omega$)**			
		Sample disc 1	**Sample disc 2**	**Sample disc 3**	**Mean ± std. error**
CSN	2.4	8.17	8.16	8.18	8.17 ± 0.01
	3.0	10.20	10.18	10.21	10.20 ± 0.01
	3.5	11.93	11.92	11.95	11.93 ± 0.01
	4.0	13.69	13.67	13.64	13.67 ± 0.02
	4.5	15.33	15.31	15.36	15.33 ± 0.02
PSN	2.4	9.21	9.24	9.18	9.21 ± 0.02
	3.0	11.51	11.53	11.56	11.55 ± 0.01
	3.5	13.41	13.45	13.42	13.43 ± 0.01
	4.0	15.69	15.67	15.71	15.69 ± 0.01
	4.5	17.26	17.25	17.29	17.27 ± 0.01
OSN	2.4	6.65	6.68	6.71	6.68 ± 0.02
	3.0	8.33	8.31	8.35	8.33 ± 0.01
	3.5	9.74	9.72	9.74	9.73 ± 0.01
	4.0	11.14	11.12	11.17	11.14 ± 0.02
	4.5	12.53	12.50	12.54	12.52 ± 0.01

A close observation of the values in Table 3 shows strong evidence that samples from PSN demonstrate the highest resistivity value, followed by that of OSN. The results collaborate with the trend in Table 2 and agree with the observation that the periwinkle shell is more electrically resistive than the Clam shell and Oyster shell. Judging from the reports that the shells have a high percentage of $CaCO_3$ as their major constituents, it is plausible that the resistive nature of the fabricated samples is influenced by the mineral contents.

Table 3. Summary of resistivity values obtained at (25.0 ± 1.0°C).

Material type	**Slope values derived from fig. 3 ($10^9\Omega m^{-1}$)**	**Computed values of resistivity, ρ ($10^5\,\Omega m$)**
CSN	3.409 ± 0.003	6.024 ± 0.009
PSN	3.861 ± 0.016	6.823 ± 0.030
OSN	2.782 ± 0.001	4.916 ± 0.007

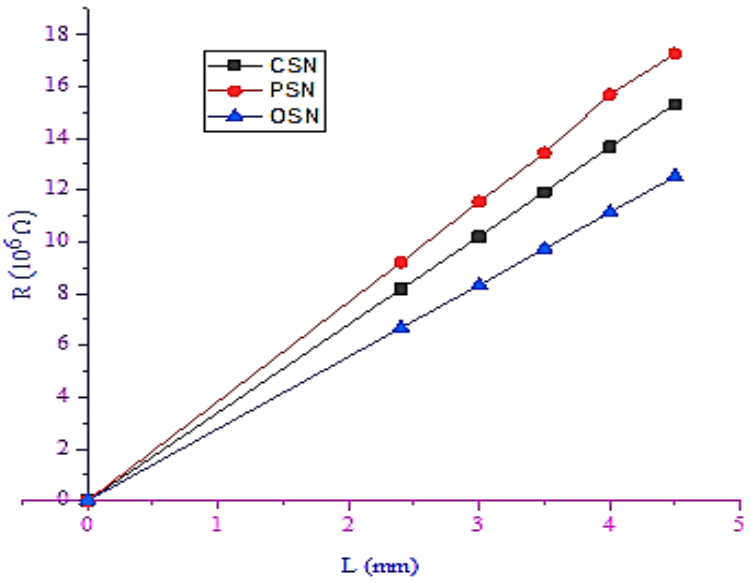

Figure 3. Variation of electrical resistance depending on samples' length.

The values in table 4 indicate that the electrical resistance decreases with an increase in temperature. For the range of temperatures considered, it can be inferred from the results that the electrical resistances of the samples fabricated using the CSN, PSN, and OSN decreased by about 91.6 %, 89.9 %, and 94.1% respectively.

Table 4. Electrical resistance vs Temperature data.

Material type	Temperature T (°C)	Electrical resistance R ($10^6\Omega$) measured for disc samples of length L = 4.0 mm			
		Sample 1	Sample 2	Sample 3	Mean ± std. error
CSN	20.0	20.93	20.94	20.96	20.94 ± 0.01
	25.0	13.69	13.67	13.64	13.67 ± 0.02
	30.0	8.68	8.72	8.69	8.70 ± 0.01
	35.0	5.72	5.75	5.71	5.73 ± 0.01
	40.0	3.80	3.84	3.82	3.82 ± 0.01
	45.0	2.55	2.60	2.58	2.58 ± 0.02
	50.0	1.78	1.75	1.75	1.76 ± 0.01
PSN	20.0	24.83	24.79	24.81	24.81 ± 0.01
	25.0	15.69	15.68	15.70	15.69 ± 0.01
	30.0	11.35	11.38	11.34	11.36 ± 0.01
	35.0	7.81	7.85	7.83	7.83 ± 0.01
	40.0	5.42	5.47	5.56	5.45 ± 0.02
	45.0	3.88	3.87	3.84	3.86 ± 0.01
	50.0	2.49	2.48	2.52	2.50 ± 0.01
OSN	20.0	18.63	18.69	18.65	18.66 ± 0.02
	25.0	11.13	11.14	11.16	11.14 ± 0.01
	30.0	7.05	7.10	7.08	7.08 ± 0.02
	35.0	4.45	4.42	4.47	4.45 ± 0.02
	40.0	2.87	2.83	2.84	2.85 ± 0.01
	45.0	1.82	1.84	1.86	1.83 ± 0.01
	50.0	1.08	1.10	1.12	1.10 ± 0.01

In figure 4, it can be observed that exponential decay is exhibited by the resistance with increasing temperature.

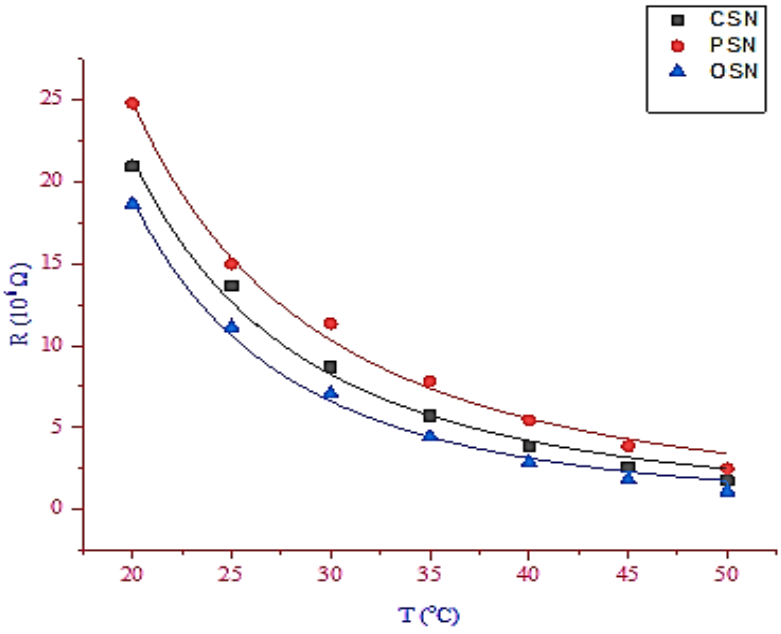

Figure 4. Variation of samples' electrical resistance depending on temperature.

However, linear relationships are observed in the cases involving how *ln R* trends with the inverse of absolute temperature as illustrated in Figure 5. These relationships agree with the empirical fact derived from eq. 11 and which can be expressed thus

$$\ln R = \ln R_o + \frac{\beta}{T} \tag{16}$$

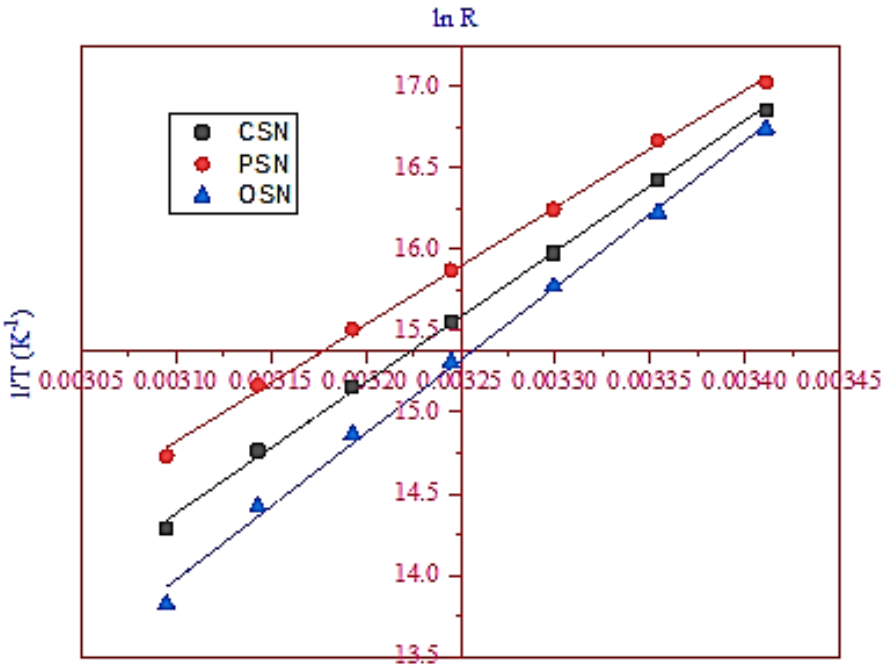

Figure 5. Plot of *ln* R against 1/T.

Table 5 summarised the results of some important electrical characteristics of the fabricated samples. The β-parameter has to do with the energy needed for the formation and transport of charge carriers that cause electrical conduction in the fabricated samples. Electronic activation energy denotes the quantity of energy required for the movement of charge carriers in the samples. The resistive ability of the samples increases with an increase in β – parameter, whereas activation energy determines intermolecular forces. It means that the higher the electrical resistance of the samples, the greater the amount of energy required to start and control conduction over the samples' insulating ability (ROBERT *et al.*, 2020).

Table 5. Summary of electrical characteristics of the test samples.

Material type	$\boldsymbol{\beta}$ $(\boldsymbol{K})$	$\boldsymbol{E_a}$ $(\boldsymbol{eV})$	$\boldsymbol{\alpha}$ $(\%/\boldsymbol{K})$	$\boldsymbol{\rho}$ $(\boldsymbol{10^5 \Omega m})$
CSN	8042	0.69	- 9.05	6.02
PSN	7189	0.62	- 8.09	6.82
OSN	8984	0.76	- 10.12	4.92

The evidence in relation to the temperature coefficient of resistance lends credence to the fact that Clam, Periwinkle, and Oyster shells are potential raw materials to produce NTC thermistors and as transducers for control.

References:

[1] ADEWUYI, A.P., ADEGOKE, T. (2008): Exploratory study of Periwinkle shell as coarse aggregates in concrete works. *ARPN Journal of Engineering and Applied Science* **3** (6): 1–6.

[2] ADEYEMO, A.O., ONUHA, G., INYANG, I. (2013): Parasitic survey of Clam (*Galatea paradoxa*) from two locations in Southern Ijaw Local Government Area of Bayelsa State, Nigeria. *Merit Research Journal of Environmental Science and Toxicology* **1** (3): 66–70.

[3] AJEI-BOATENG, D., AMISAH, S., QUAGRAINLE, K.K. (2009): Bacteriological contamination of the freshwater Clam (*Galatea paradoxa*) from the Volta estuary. Ghana. *African Journal of Microbiology Research* **3** (7): 396–399. doi: 10.5897/AJMR.9000121

[4] AKINJOGUNLA, V.F., MORUF, R.O. (2018): The ecology and growth biology of *Farfantepenaeus notialis* (Pérez-Farfante, 1967) from an open tidal estuary in Nigeria. *Nigerian Journal of Fisheries* **15** (1): 1326–1335.

[5] ASTM D6393 (2021): Standard Test Method for Bulk Solids Characterization by Carr's Indices, ASTM International, West Conshohocken, PA.

[6] ATUANYA, C.U., EDOKPIA, R.O., AIGBODION, V.S. (2014): The Physio-mechanical properties of recycle low density polyethylene/bean pod ash particulates composites. *Results in Physics* **4**: 88–95. doi: 10.1016/j.rinp.2014.05.003

[7] BUNJAMIN, B., MUKHLIS, A. (2020): Utilization of Oyster shells as a substitute part of cement and fine aggregate in the compressive strength of concrete. *Aceh International Journal of Science and Technology* **9** (3): 150–156. doi: 10.13170/aijst.9.3.17761

[8] COLOMA, L.C., FANUGA, L.N., OCRETO, C.A., RODRIGUEZ, R.C. (2006): Calcium Fluoride (CaF_2) from Oyster shell as a Raw Material for Thermoluminescence Dosimeter. A Thesis in partial fulfilment of the requirements for the degree of Bachelor of Science in Physics,

presented to the Department of Natural Sciences, College of Science, Polytechnic University of the Philippines. Available at: https://inis.iaea.org/collection/NCLCollectionStore/_Public/37/055/37055011.pdf

[9] EHIGIATOR, F.A.R., OSAWARU, R., (2016): Shell growth pattern of the freshwater Clam (*Egeria radiata*) in the Forcados River, Niger Delta, Nigeria. *Nigerian Journal of Agriculture, Food and Environmental*, **12** (2): 92–97.

[10] EKPE, S.D., DEW, S.K. (2002): Investigation of thermal flux to the substrate during sputter deposition of aluminium. *Journal of Vaccum Science and Technology* **A20** (6): 1877–1885. doi: 10.1116/1.1507342

[11] EKPE, S.D., DEW, S.K. (2004): Measurement of Energy flux at the substrate in a Magnetron Sputter System using an integrated sensor. *Journal of Vaccum Science and Technology*, **A22** (4): 1420–1424. doi: 10.1116/1.1705640

[12] EKPE, S.D. (2005): Study of energy flux in a magnetron sputter deposition system. *PhD Thesis*, Faculty of Graduate Studies and Research, Department of Electrical and Computer Engineering, University of Alberta, Edmonton, Alberta, p. 63.

[13] ETUK, S.E., EMAH, J.B., ROBERT, U.W., AGBASI, O.E., AKPABIO, I.A. (2021): Comparison of electrical resistivity of soots formed by combustion of kerosene, diesel, aviation fuel and their mixtures. *Brilliant Engineering* **3**: 6–10. doi: 10.36937/ben.2021.003.002

[14] HAMESTER, M.R.R., BALZER, P.S., BECKER, D. (2012): Characterization of calcium carbonate obtained from oyster shells and incorporation in polypropylene. *Materials Research* **15** (2): 204–208.

[15] KIM, W., SINGH, R., SMITH, J.A. (2020): Modified crushed oyster shells for fluoride removal from water. *Scientific Reports* **10**: 5759. doi: 10.1038/s41598-020-60743-7

[16] KINGDOM, T., ALISON, M.E., GBENEFADEL, P. (2012): Shell growth of fresh water Clam (*Galatea paradoxa*) in Ikebiri creek, Bayelsa State, Nigeria. *International Journal of Applied Research and Technology* **1** (6): 215–219.

[17] LIANG, Y., ZAO, Q., LI, X., ZHANG, Z., REN, L. (2016): Study of the microstructure and mechanical properties of white Clam shell. *Micron* **87**: 10–17. doi: 10.1016/j.micron.2016.04.007

[18] LUO, W., YAO, H.M., YANG, P.H., CHEN, C.S. (2009): Negative temperature coefficient material with low thermal constant and high resistivity for low temperature thermistor application. *Journal of the American Ceramic Society* **92** (11): 2682–2686. doi: 10.1111/j.1551-2916.2009.03289.

[19] MA, Y., CHAI, X., YAN, Z., CHEN, D., MAN, J. (2012): Clam shell compression characteristics and bond strength. *Advanced Materials Research* **472**–**475**: 2554–2557. doi: 10.4028/www.scientific.net/amr.472-475.2554

[20] MORRIS, N.M. (1996): *Mastering Electronic and Electrical calculation*. Macmillan Press Ltd, London.

[21] MUNIFAH, S.S., WIENDARTUN, AMINUDIM, A. (2018): Design of temperature measuring instrument using NTC thermistor of Fe_2TiO_5 based on microcontroller AT mega 328. *Journal of Physics: Conference Series* **1280** (2): 022052 doi: 10.1088/1742-6596/1280/2/022052

[22] OBOT, M.U., YAWAS, D.S., AKU, S.Y. (2017): Development of an abrasive material using Periwinkle shells. *Journal of King Saud University – Engineering Sciences* **29** (3): 284–288. doi: 10.1016/j.jksues.2015.10.008.

[23] ONUOHA, C., ONYEMAOBI, O.O., ANYAKWO, C.N., ONUEGBU, G.C. (2017): Physical and morphological properties of Periwinkle shell – filled recycled polypropylene composites. *International Journal of Innovative Science, Engineering and Technology* **4** (5): 186–196.

[24] ROBERT U.W., ETUK, S.E., AGBASI, O.E., IBOH, U.A., EKPO, S.S. (2020): Temperature-dependent electrical characteristics of disc-shaped compacts fabricated using calcined eggshell nano powder and dry cassava starch. *Powder Metallurgy Progress* **20** (1): 12–20. doi: 10.2478/pmp-2020-0002

[25] SEDHA, R.S. (2008): *A Textbook of Applied Electronics*, Multicolor Revised Edn., S. Chand & Company Ltd, Ram Nagar, New Delhi, India.

[26] SCHERZ, P., MONK, S. (2016): Practical electronics for inventors, 4th Edn., McGrawHill Education, New York. 25–28.

[27] THERAJA, B.L., THERAJA, A.K. (2005): A Textbook of Electrical Technology, Multicolor Illustrative Edn., S. Chand & Company Ltd, Ram Nagar, New Delhi, India. 2041 pp.

[28] THERAJA, B.L. (2012): Basic Electronics: Solid State, Multicolor Illustrative Edn., S. Chand & Company Ltd, Ran Nagar, New Delhi, India. 172 pp.

[29] TUROLLA, E., CASTALDELLI, G., FANO, E.A., TAMBURINI, E. (2020): Life cycle assessment (lca) proves that manila clam farming (*Ruditapes philippinarum*) is a fully sustainable aquaculture practice and a carbon sink. *Sustainability* **12** (13): 5252. doi: 10.3390/su12135252

[30] YOUNG, H.D., FREEDMAN, R.A. (2008): *University Physics with Modern Physics*. Pearson International Edn., Pearson Addison Wesley, New York. 850–854.